International Journal of Renewable Energy Resources 13 (2023) 58-75
https://doi.org/10.22452/ijrer.vol13no2.3

CARBON MONOXIDE-RESISTANT ANODE CATALYSTS FOR SINGLE-CELL DIRECT CARBON MONOXIDE FUEL CELLS: BINARY, TERNARY, AND QUATERNARY PLATINUM ALLOYS AS ANODE ELECTROCATALYSTS

Farshid Zabihian[1,*], Asad Davari[2] & Gifty Osei-Prempeh[3]
[1]Department of Mechanical Engineering, California State University Sacramento, Sacramento, CA, U.S.A.
[2]Electrical & Computer Engineering Department, West Virginia University Institute of Technology, Beckley, WV, U.S.A.
[3]Chemical Engineering Department, West Virginia University Institute of Technology, Beckley, WV, U.S.A.
*e-mail: farshid.zabihian@csus.edu

Abstract
The objective of this paper is to present the results of experimentations on the custom-made anode electrocatalysts for direct carbon monoxide fuel cells (DCMFCs) inspired by catalysts commonly used for direct alcohol fuel cells. Seven different catalysts were fabricated and tested. The uniform and consistent manufacturing process and the test procedure allowed a meaningful comparison of the developed fuel cells. The results indicated that homemade Pt-Ru membrane-electrode assembly (MEA) could not compete with the Pt-Sn MEA. While the performance of the MEAs with Pt-Ru-Ni, Pt-Ru-Sn-Ni, and Pt-Ru-Sn-Co was not satisfactory, the Pt-Ru-Sn-Co-W MEA achieved the best performance among all MEAs with Nafion® 117 membrane. The last MEA was made of the Pt-Sn anode catalyst and Nafion® 212 membrane and outperformed all other MEAs by a wide margin. The experiments demonstrated that the performance of the best-developed MEA was three times better than the performance of the commercial Pt-Ru MEA. This means the performance of DCMFCs can be significantly improved by developing a suitable anode electrocatalyst, using a thinner membrane, and operating at optimum conditions. These results are not only applicable for DCMFCs but also are very useful for other proton exchange membrane fuel cells (PEMFCs) operating with CO-containing fuels.

Keywords: Fuel Cell; Carbon Monoxide; Catalysts; Platinum Alloys; Coal

1. INTRODUCTION

Coal is playing and will continue to play a major role in the electricity generation industry in many countries throughout the world; therefore, it is vital to improve the sustainability of this industry by improving the efficiency of coal-powered electricity generation systems and reducing their environmental impacts. While theoretically, direct carbon fuel cells (DCFCs) are a prime candidate to efficiently convert the chemical energy of coal to electricity by fuel cells, they are facing major technical challenges. An alternative approach is to process coal and other carbon-bearing fuels into gaseous fuels before feeding them to fuel cells. This conversion can be achieved via either the gasification process or partial oxidation (POX) process. While the gasification process is industrially developed, it needs a significant amount of water, which makes it unsuitable for portable applications. On the contrary, the POX process in the form of sub-stoichiometric combustion does not require any water and is simple. These characteristics make the POX process an ideal choice for this particular application. The produced gas, which contains a high concentration of carbon monoxide, can be fed to proton exchange membrane fuel cells (PEMFCs). However, typically, platinum-based catalysts are used to make electrodes in this type of fuel cell which can be poisoned in the presence of CO in the anode. So, the development of direct carbon monoxide fuel cells (DCMFCs) requires electrocatalysts with high resistance to CO poisoning. Since a similar problem exists for direct alcohol fuel cells (DAFCs), including direct methanol fuel cells (DMFC), direct ethanol fuel cells (DEFC), and direct formic acid fuel cells (DFAFC), the catalysts developed for these fuel cells are used as an inspiration in this research. This is because during the alcohol reforming process, carbon monoxide is generated and the electrocatalyst of these fuel cells must also cope with the problem of CO poisoning. While several solutions have been proposed to address this problem, the most practical and common approach is to use transition metals to form a platinum alloy as anode electrocatalysts for fuel cells.

For this purpose, one, two, or even more other metals have been added to platinum to create CO-resistant catalysts.

The originality of this paper stems not only from the novelty of the idea of feeding PEMFCs with carbon monoxide-containing fuels but also from the comparability of the results of a wide variety of electrocatalysts that were developed and tested at similar conditions.

2. METHODOLOGY

In this paper, the development and testing of several binary alloys of Pt and other metals to electrooxidize carbon monoxide are presented. This is followed by several ternary and quaternary alloys of platinum. The procedure to create electrocatalysts and manufacture MEAs, and the test procedure were presented in details in the companion paper (Zabihian et al., 2023). The anodic electrocatalyst preparation process included dissolving metal precursors in Ethylene Glycol, adding KOH solution, synthesizing by the reduction process after the addition of $NaBH_4$, and filtering, washing, and drying the solid catalyst particles. For the carbon-supported catalysts, Vulcan was added. The anodic and cathodic catalyst solutions were created by mixing the Nafion® solution and water with the anode catalyst and Pt black, respectively. The anodic and cathodic catalyst solutions were painted on 5 cm^2 carbon papers and allowed to dry. To creat membrane-electrode assembly (MEA), a Nafion® membrane was sandwiched between the painted carbon papers using the hot-press process for the duration of six minutes at 140°C. Initially, Nafion®117 by DuPont and later Nafion®212 (to improve the power density of the fuel cell) were employed. D521 and D1021 Nafion® dispersions, manufactured by Ion Power Inc., were used as the binders. To test the manufactured MEAs, an 850e Fuel Cell Test System (Scribner), a fully automated computer-controlled system, was used. The station can automatically create the polarization curve of MEAs at controlled cell operating temperatures, mass flow rates of fuel and oxidant, and temperature of humidifiers (both anode and cathode flows) using different fuels and oxidants.

For simplification, throughout this paper, the manufactured MEAs are identied by their membrane, anode, and cathode materials (or anode and cathode materials). For example, N117/Pt-Sn/Pt or Pt-Sn/Pt represents an MEA made of platinum (Pt) – tin (Sn), platinum (Pt), and Nafion®117 as the anode electrocatalyst, cathode electrocatalyst, and the electrolyte membrane, respectively. A similar notification is used to express the temperatures of the MEA, and anode and cathode humidification flows (e.g. 90/80/95°C).

3. RESULTS AND DISCUSSION

3.1 Binary Alloys of Pt and Metals Other Than Ru

Ruthenium (Ru) is not the only metal that can be alloyed with Pt as electrocatalysts. Other metals have been tried with varying success levels, including the Pt-alloy with

- molybdenum (Mo) (Torres-Santillan, et al., 2022; Molochas & Tsiakaras, 2021; Pillai, et al., 2019; Wang et al., 2007; Santiago et al., 2003; Samjeské et al., 2002; Neto et al., 2002; Grgur et al., 1998; Mukerjee et al., 1999),
- tin (Sn) (Sapkota et al., 2023; Di et al., 2022; Zhang et al., 2021; Goel & Basu, 2012; Simões et al., 2007; Colmati et al., 2006; Rousseau et al., 2006; Song et al., 2005; Vigier et al., 2004a; Jiang et al., 2004; Zhou et al., 2004; Vigier et al., 2004b; Pick, 1999; Götz & Wendt, 1998),
- cobalt (Co) (Lin et al., 2022; Liang et al., 2019; Antolini et al., 2006),
- iron (Fe) (Zhang et al., 2022; Litkohi et al., 2020; Yang et al., 2019; Xu et al., 2006; Li et al., 2004),
- tungsten (W) (Zhou et al., 2004; Ham et al., 2008),
- nickel (Ni) (Litkohi et al., 2020; Yang et al., 2019; Antolini et al., 2006; Choi et al., 2003),
- gold (Au) (Latif et al., 2020; Lee et al., 2008),
- osmium (Os) (Santos & Tremiliosi-Filho, 2003),
- iridium (Ir) (Li et al., 2023; Gurau et al., 1998),
- rhenium (Re) (Goel & Basu, 2012; Vigier et al., 2004b),
- and lead (Pd) (Yang et al., 2019; Li & Pickup, 2006; Zhou et al., 2004).

Also, metal oxides have been added to Pt to fabricate electrocatalysts, including

- MoO_x (Kurdin et al., 2022; Ioroi et al., 2002; Wang et al., 2001; Zhang et al., 1999),
- WO_3 (Tian et al., 2021; Brkovic et al., 2020; Antolini, 2007; Shen et al., 1995),
- NbO_x (Ueda et al., 2003),
- TaO_x (Gao et al., 2019; Ueda et al., 2003),
- SnO_x (Dubau et al., 2020; Spasov et al., 2019; Jiménez-Morales et al., 2019; Matsui et al., 2006),
- PbO_x (Suffredini et al., 2007),
- RuO_2 (Lee et al., 2021a; Eguiluz et al., 2010),
- RhO_2 (Eguiluz et al., 2010),
- IrO_2 (Ahn et al., 2022; Moore et al., 2019).
- ReO_x (Kim et al., 2022)

The general conclusion of most of these studies was that these catalysts typically were better catalysts than pure Pt in terms of both electrochemical activities and CO tolerance. But their performance was inferior compared to that of Pt–Ru and Pt–Sn catalysts. One of the most promising and most studied Pt-based catalysts is platinum-tin (Pt-Sn) alloy. Therefore, this catalyst will be investigated next.

3.1.1. Platinum (Pt) – Tin (Sn) Electrocatalysts

Among many attempted binary Pt-based catalysts, the Pt–Sn catalysts have the most potential to replace Pt–Ru catalysts. It has been reported that Pt-Sn catalysts have better CO tolerance compared to Pt-Ru alloys (Di et al., 2022; Matsui et al., 2006; Goel & Basu, 2012). Rousseau et al. (2006) reported that alloying platinum and tin in a carbon-supported electrocatalyst improved the catalytic activity of carbon-supported Pt from a few mW/cm^2 to about 30 mW/cm^2 at 80°C in a direct ethanol fuel cell (DEFC). Di et al. (2022) studied various combinations of Pt-Sn catalysts (Pt_xSn_y with x=3, 1, 1, 1 and y=1, 1, 2, 4). They reported that the performance of all electrocatalysts was superior to that of the commercial Pt/C. They also showed that x=1 and y=1 had the best performance and stability. Zhou et al. (2004) demonstrated the superior performance of carbon-supported Pt-Sn catalysts compared to carbon-supported Pt-Ru, Pt-W, Pt-Pd, and Pt catalysts in a single DEFC. The maximum power density of Pt-Sn doubled that of the second-best performing catalyst, Pt-Ru. Jiang et al. (2004) reported that the catalyst preparation method affects the tin oxidation state and thus the electrochemical activity of the catalyst. Simões et al. (2007) developed and tested various Pt-Sn catalysts for DEFCs. They developed their DEFC using carbon-supported Pt-Sn as the anode catalyst, Pt as the cathode catalyst, and Nafion® 117 as the electrolyte. While based on the electrochemical characterization, they reported Pt 60% - Sn 40% as the best catalyst in terms of activity for ethanol oxidation, the catalyst with the highest power density (when used to create the MEA for a DEFC) was Pt 90% - Sn 10%. They attributed this apparent discrepancy to different temperatures during the electrochemical characterization (room temperature) and the operation of the fuel cell.

In this MEA, first, several tests were conducted to evaluate the performance of the fuel cell when fed with CO-N_2 and CO as the fuel, and air and oxygen as the oxidant at the operating temperature of 80°C. Fig. 1 shows that the fuel cell fueled with CO and O_2 outperformed other cases (with the maximum power density of 59.4 mW/cm^2) followed by when the fuel cell was fueled with CO and air (with the maximum power density of 49.2 mW/cm^2). The worst performance was when it was fueled with CO-N_2 and air (with the maximum power density of 44.7 mW/cm^2). The performance of the MEA at lower current densities was close but with an increase in current densities, the differences grow. It should be noted that in these experiments the flow rates of the fuels and oxidants varied, 50/100 mlit/min for CO/O_2, 50/250 mlit/min for CO/air, and 250/1500 mlit/min for CO-N_2/air. In all these cases, the maximum power densities were significantly higher than the values reported by Rousseau et al. (2006) for Pt-Sn catalysts used in their DEFCs at the same operating temperature (about 30 mW/cm^2).

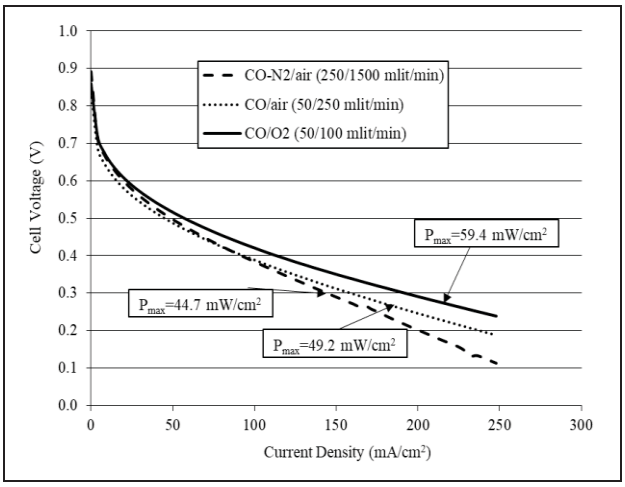

Fig. 1. The polarization curves of MEA with Pt-Sn anode catalyst fed with the mixture of CO-N_2 and CO as the fuel and air and O_2 as the oxidant (at the operating temperature of 80°C): The effects of the fuel and oxidant composition.

To investigate the impacts of the operating temperature on the fuel cell performance, the experiments were conducted using the mixture of CO-N_2 as the fuel and air as the oxidant with various flow rates (as shown in the diagram) at the operating temperatures of 80 to 95°C with the increment of 5°C. The curves in Fig. 2 show that at the high operating temperatures of 90 and 95°C, the fuel cell operation was unstable probably due to the drying effect on the electrolyte. The maximum power densities of the cell at 80, 85, and 95°C were 44.7, 44.5, and 43.8 mW/cm^2, respectively. Lamy et al. (2004) reported the power density of about 20 mW/cm^2 at the operating temperature of 90°C and about 27 mW/cm^2 at the operating temperature of 110°C for the Pt-Sn catalyst in a DEFC. While the developed Pt-Sn catalyst for this paper outperformed the reported results by Lamy et al. (2004), it did not demonstrate the expected strong dependency on operating temperatures. This might be because of the high operating temperatures of the MEA (close to the upper limits of the operating temperature of the membrane). Also, they reported an open circuit voltage (OCV) of 0.72 V which is much lower than that of the developed MEA in this research at about 0.9 V. However, in both the developed MEA and the reported results by Lamy et al. (2004), the OCVs are unaffected by the operating temperatures.

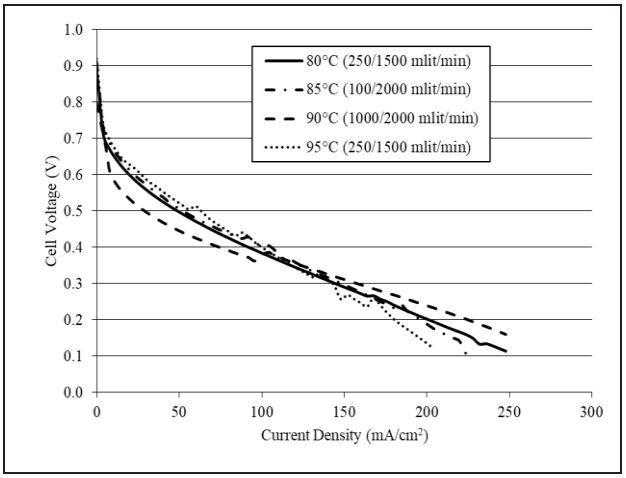

Fig. 2. The polarization curves of MEA with Pt-Sn anode catalyst fed with the mixture of CO-N_2 as the fuel and air as the oxidant: The effects of the operating temperature.

Comparing the maximum power density of the current MEA with that of the commercial Pt-Ru DMFC when fueled with the mixture of CO-N_2 and air at the operating temperature of 80°C (approximately 45 vs. 24 mW/cm^2, respectively) indicates that the homemade MEA with the unsupported Pt-Sn anode catalyst had a significantly better performance than that of the commercial Pt-Ru MEA. Similarly, when fed with CO and O_2 at the operating temperature of 80°C, the homemade MEA with the unsupported Pt-Sn anode catalyst performed much better than the homemade MEA with the unsupported Pt-Ru anode catalyst (approximately 60 vs. 34 mW/cm^2, respectively). Comparing the performance of the homemade MEA with the unsupported Pt-Sn and Pt-Ru anode catalysts when fed with CO-N_2 and air at the operating temperature of 95°C indicates similar results but with a smaller difference (approximately 44 vs. 39 mW/cm^2, respectively).

The superior performance of the fuel cell with the anode catalyst of Pt-Sn compared to that of the fuel cell with the anode catalyst of Pt-Ru confirms the similar results reported by Zhou et al. (2004) for DEFCs although they reported a larger difference in some cases. Similar results are reported by others such as Zhou et al. (2003), Song et al. (2005), Colmati et al. (2006), and Zhou et al. (2004). It should be noted that the reported results on the superiority of Pt-Sn anode catalyst were only for DEFCs. For DMFCs, fuel cells with the anode catalyst of Pt-Ru have reportedly superior performance compared to that of fuel cells with the anode catalyst of Pt-Sn (Zhou et al., 2003; Song et al., 2005; and Colmati et al., 2006).

3.1.2. Vulcan-Carbon Nanotubes-Supported Pt-Sn Electrocatalyst

Catalyst supports are added to electrocatalysts to improve their catalytic activity, ionic and electronic conductivity, and porosity. It was shown that the addition of carbon support (Vulcan) did not improve the performance of the Pt-Ru anode catalyst. In this section, the impact of the addition of support to the Pt-Sn anode catalyst will be investigated. The anode electrode of the fabricated MEA was the Vulcan-carbon nanotubes (CNT)-supported Pt-Sn with the catalyst loading of 6 mg/cm^2 and the cathode electrode was the carbon-supported platinum with the loading of 4 mg/cm^2 and Nafion® 117 as the electrolyte.

In these experiments, first, the effect of the fuel type is investigated. Fig. 3 shows the polarization curves of the fuel cell when fueled with CO-N_2 (20% and 80% volume-based, respectively) and H_2 as the fuel and oxygen as the oxidant with the flow rates of 100/200 mlit/min at the operating temperature of 80°C. The ratio of the maximum power density of the fuel cell when fueled with hydrogen to that of the CO-N_2-fueled fuel cell was 12.8 (136 vs 10.6 mW/cm^2, respectively).

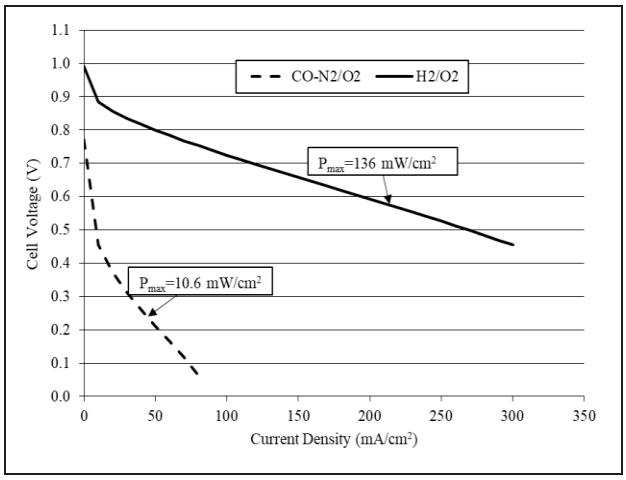

Fig. 3. The polarization curves of the MEA with the carbon-supported Pt-Sn anode catalyst fed with the mixture of CO-N_2 and hydrogen as the fuels and oxygen as the oxidant: The effect of the fuel type.

Fig. 4 depicts how the fuel cell operating temperature influences the performance of the cell when it was fueled with hydrogen and oxygen with the flow rates of 100 and 200 mlit/min, respectively, at two temperatures, 40 and 80°C. The curves show that the maximum power density of the cell increases from 108 to 136 mW/cm^2 when the operating temperature increases from 40 to 80°C. The difference between the two curves becomes more significant with an increase in current density.

Similarly, Fig. 5 illustrates the polarization curves of the fuel cell when fueled with CO-N_2 and O_2 (100/200 mlit/min) at the operating temperatures of 80 and 95°C. Remarkably, the figure indicates that the maximum power density of the fuel cell more than doubled when the operating temperature increased from 80 to 95°C. For comparison, the ratio of the maximum power density of the fuel cell when fed by hydrogen and oxygen (Fig. 4) increased by about 26% when the operating temperature increased from 40 to 80°C.

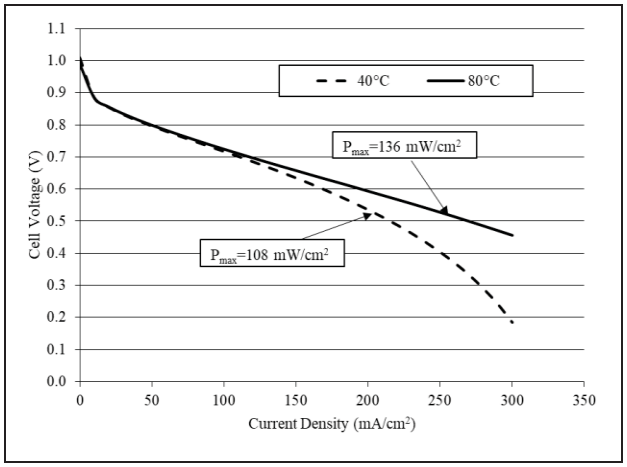

Fig. 4. The polarization curves of the MEA with the carbon-supported Pt-Sn anode catalyst fed with hydrogen as the fuel and oxygen as the oxidant (100/200 mlit/min): The effect of the operating temperature.

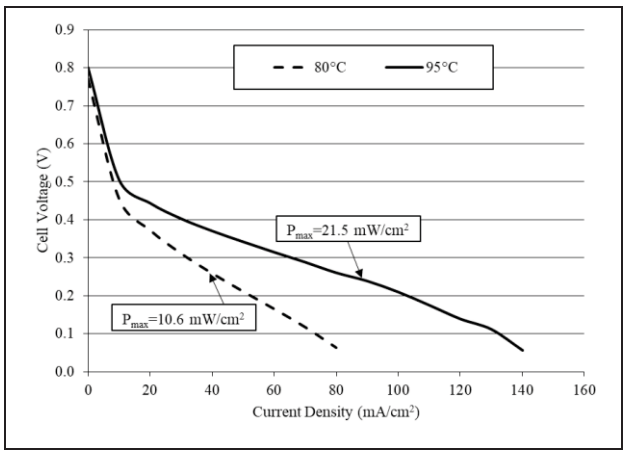

Fig. 5. The polarization curves of the MEA with the carbon-supported Pt-Sn anode catalyst fed with CO-N_2 as the fuel and O_2 as the oxidant (100/200 mlit/min): The effect of the operating temperature.

Fig. 6 depicts the effect of the fuel and oxidant flow rates on the performance of the fuel cell at two operating temperatures, 80 and 95°C. The curves show that at the operating temperature of 80°C, the performances of the fuel cell with various flow rates are close. But at the operating temperature of 95°C, increasing the flow rates significantly improves the performance of the fuel cell. The reason can be because of the higher activity of the electrocatalyst at the higher temperature which increases the rate of reactions. This means at the high operating temperature and the low flow rate, the cell is starved. This behavior is different from what was previously observed for the MEA with Pt-Sn anode catalyst fed with the mixture of CO-N_2 as the fuel and air as the oxidant (Fig. 2). This might be an indication that the MEA with the carbon-supported Pt-Sn anode catalyst has some room for further performance improvement.

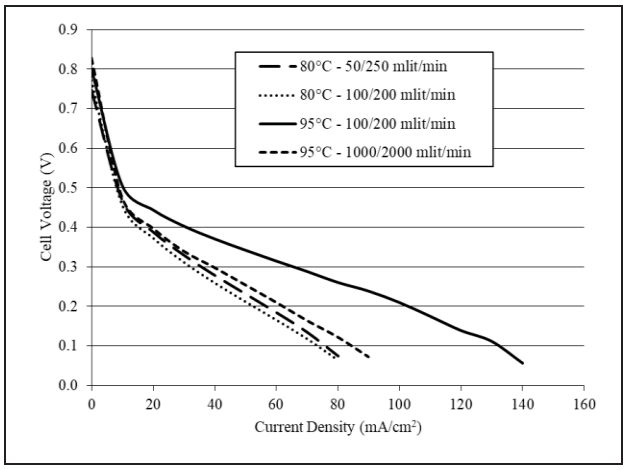

Fig. 6. The polarization curves of the MEA with the carbon-supported Pt-Sn anode catalyst fed with CO-N_2 as the fuel and O_2 as the oxidant: The effect of the fuel and oxidant flow rates.

The comparison of the experimental results for the carbon-supported Pt-Ru and Pt-Sn anode electrocatalysts indicates that the performance of the two MEAs is consistent when fed with CO and O_2. At the operating temperature of 80°C, the power density of 10 to 13 mW/cm^2 and at the operating temperature of 95°C the power density of 18 to 22 mW/cm^2 were observed in these two catalysts. For hydrogen/oxygen-fed MEAs at the operating temperature of 80°C, the power densities of 194 and 136 mW/cm^2 were achieved for the carbon-supported Pt-Ru and Pt-Sn anode catalysts, respectively. However, the comparison of the performance of the MEAs made of the supported and unsupported Pt-Sn anode catalysts indicates a significantly inferior performance of the former. The power densities of the supported and unsupported Pt-Sn anode catalysts when fueled with CO-N_2 at the operating temperature of 80°C were approximately 10 and 45 mW/cm^2, respectively. In fact, the carbon-supported

Pt-Sn anode catalyst had the worst performance among all the developed and tested anode catalysts (Liu et al., 1998).

3.2. Adding Other Metals to Pt-Ru

Many researchers have tried to add a third metal to a Pt-Ru catalyst to create a ternary catalyst anticipating an improvement in the electrochemical characteristics of the catalyst as well as reducing the consumption of platinum and ruthenium (Yang et al., 2021).

It is reported that in the ethanol oxidation reaction, most ternary Pt–Ru-based and Pt–Sn-based electrocatalysts outperformed Pt–Ru and Pt–Sn electrocatalysts (Antolini, 2007). However, some of these catalysts have suffered from problems due to the lack of durability and stability (Wang et al., 2007). Some of the ternary Pt–Ru, Pt-Sn, and Pt-Ni based electrocatalysts reported in the literature are listed in Table 1. It should be noted that some researchers added metal oxides to create anode electrocatalysts.

Table 1: The list of articles in the literature that studied multiple-metal anode electrocatalysts

Anode electrocatalysts	Pt-Ru	Pt-Sn	Pt-Ni
Sn	Hang et al., 2020; Rousseau et al., 2006; Aramata & Masuda, 1991; Zhou et al., 2004		
Ni	Lee et al., 2021b; Wang et al., 2006; Choi et al., 2003; Pasupathi & Tricoli, 2008; Zhou et al., 2004; Ye et al., 2007; Martínez-Huerta et al., 2006		
Mo	Gonzalez-Hernandez et al., 2020; Pasupathi & Tricoli, 2008; Zhao et al., 2014; Zhou et al., 2003		
W	Zhou et al., 2003; Zhou et al., 2004		Wang et al., 2023
Os	Ley et al., 1997; Chu & Jiang, 2002	Goel & Basu, 2012	
Co	Mukherjee et al., 2022; Pasupathi & Tricoli, 2008; Zhang et al., 2004; Moreno et al., 2009		
Pb	Li & Pickup, 2006		
Pd	He et al., 1997		
Ir	Ravichandran et al., 2022; Pasupathi & Tricoli, 2008	Goel & Basu, 2012	Lin et al., 2020
Re	Choudhary & Pramanik, 2020	Goel & Basu, 2012	
Fe			Litkohi et al., 2020
WO_3	Shen et al. 1995; Jusys et al., 2002; Lasch et al., 1999		
MoO_x	Jusys et al., 2002; Lasch et al., 1999		
VO_x	Jusys et al., 2002; Lasch et al., 1999		
SnO_x	Matsui et al., 2006		

3.2.1. Pt-Ru-Ni Electrocatalysts

Wang et al. (2006) experimentally demonstrated that the catalytic activity and CO tolerance of carbon-supported Pt–Ru–Ni anode electrocatalysts were higher than those of the carbon-supported Pt-Ru. Similar results were reported by Ye et al. (2007) and Martínez-Huerta et al. (2006) for the higher catalytic activity and stability of the CNT-supported Pt-Ru-Ni catalysts in DMFCs. However, Pasupathi and Tricoli (2008) reported that the addition of “even trace amounts of nickel” in Pt-Ru anode electrocatalysts deteriorated the performance of DMFCs and reduced the catalytic activities of the catalysts toward methanol. The reason for this discrepancy might be the different fabrication methods used in these studies. While most studies used the chemical reduction method to synthesize catalysts, Pasupathi & Tricoli (2008) used the vapor deposition of Ni-precursor onto Pt-Ru catalysts for this purpose.

For this part, the anode electrocatalyst was made of the Pt-Ru-Ni with the loading of 6 mg/cm^2, and the cathode electrocatalyst was made of carbon-supported platinum with the loading of 4 mg/cm^2 and Nafion® 117 as the electrolyte. To evaluate the performance of the developed Pt-Ru-Ni MEA, first, the polarization curves when the cell was fueled with hydrogen are presented. Fig. 7 illustrates the effect of the operating temperature of the cell on the

polarization curves when the cell was fed with hydrogen as the fuel and oxygen as the oxidant (flow rates of 100/200 mlit/min) at the operating temperatures of 40 and 80°C. Similar to previous cases, the fuel cell performance was improved with an increase in the operating temperature. Comparing the performance of this MEA and those of the commercial and homemade Pt-Ru anode catalyst MEAs in similar operating conditions (the maximum power densities of 184 vs. 278 and 208 mW/cm^2, respectively, at an operating temperature of 40°C) indicates that when fueled with hydrogen, the Pt-Ru-Ni MEA performance was inferior to the Pt-Ru MEA performance for both the homemade and the commercial ones. However, the Pt-Ru-Ni outperformed the carbon-supported Pt-Ru and the carbon-supported Pt-Sn with a wide margin when fed with hydrogen and oxygen at the operating temperature of 80°C (the maximum power densities of 304 vs 194 and 136 mW/cm^2, respectively).

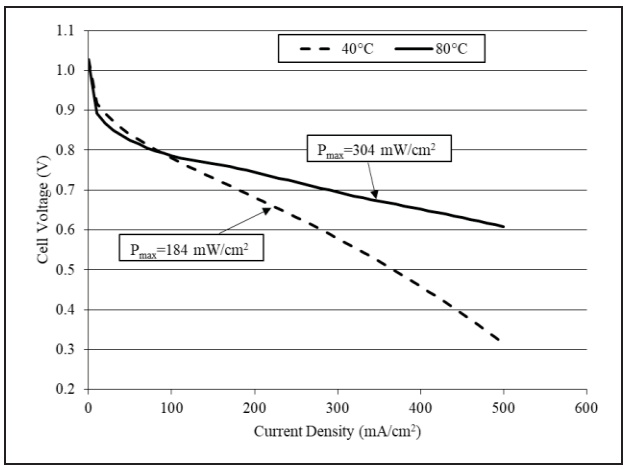

Fig. 7. The polarization curves of the Pt-Ru-Ni MEA fed with H_2 and O_2 (100/200 mlit/min): The effect of the operating temperature.

Fig. 8 depicts the effect of the oxidant flow rate, in this case, air, on the performance of the fuel cell when it is fueled with hydrogen at the operating temperature of 80°C. Increasing the air flow rate from 200 mlit/min to 1000 mlit/min improved the performance of the single cell. This improvement was manifested in the maximum power density which increased from 192 to 215 mW/cm^2. Unlike other similar cases where at low current densities the difference was very small but with an increase in current density this difference grows, in this diagram, the significant difference can be observed even at low current densities. This indicates the especially important role of oxidant air flow rate for this fuel cell.
In Fig. 7 and Fig. 8 the fuel cell was fueled with hydrogen. Next, the fuel cell performance when fueled with different fuels is investigated (Fig. 9 and Fig. 10). First, the performance of the fuel cell is compared when it is fueled with hydrogen and carbon monoxide as the fuel and oxygen as the oxidant (Fig. 9). The maximum power density of the fuel cell, when fueled with hydrogen, was about 6.4 times greater than that of when fueled with carbon monoxide (304 vs 47.4 mW/cm^2, respectively). This ratio is much lower than the same ratio for Pt-Ru MEA. The open circuit voltage of the fuel cell when fueled with hydrogen was about 1.0 V while it was about 0.8 V when fueled with carbon monoxide.

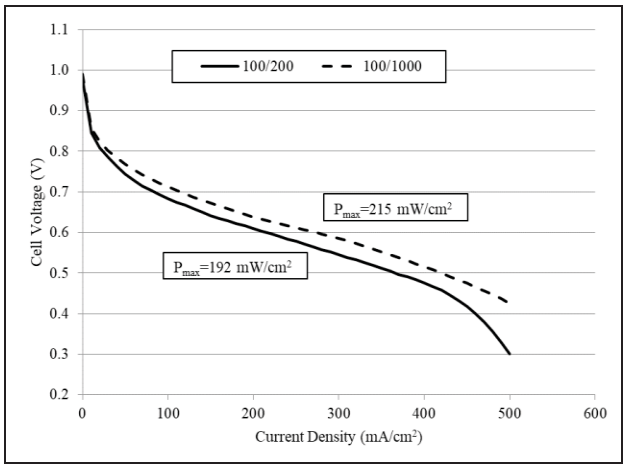

Fig. 8. The polarization curves of the Pt-Ru-Ni MEA fed with H_2 and air (at the operating temperature of 80°C): The effect of air flow rate.

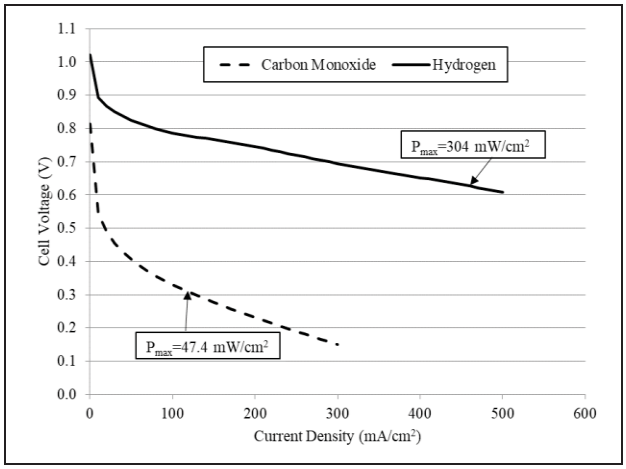

Fig. 9. The polarization curves of the Pt-Ru-Ni MEA fed with oxygen (200 mlit/min): The effect of the fuel type, H_2 and CO (100 mlit/min), at the operating temperature of 80°C.

Comparing the maximum power density of the fuel cell in Fig. 9 (CO/O_2, 100/200 mlit/min, 80°C) with that of the supported and unsupported Pt-Ru MEAs

reported at similar operating conditions, 47.4 vs. 33.2 and 12.6 mW/cm^2, respectively, indicates that in this operating condition, this MEA outperforms the Pt-Ru MEAs. However, the maximum power density of the unsupported Pt-Sn MEA (59.4 mW/cm^2) was higher than that of the supported Pt-Ru-Ni MEA. Similarly, Fig. 10 compares the performance of the fuel cell when fueled with the mixture of CO and N_2 (20% and 80% volume-based, respectively) and hydrogen as the fuel and air as the oxidant at the operating temperature of 80°C. In this case, the ratio of the maximum power density of the fuel cell when fueled with hydrogen to that when fueled with CO-N_2 was about 4.6. It should be noted that the air flow rate for hydrogen was 200 mlit/min while the flow rate for CO-N_2 was 500 mlit/min. When the air flow rate for hydrogen fuel was increased to 1000 mlit/min, the ratio increased to about 5.5. Again, as noted earlier, this indicates the importance of the oxidant flow rate for the performance of this fuel cell.

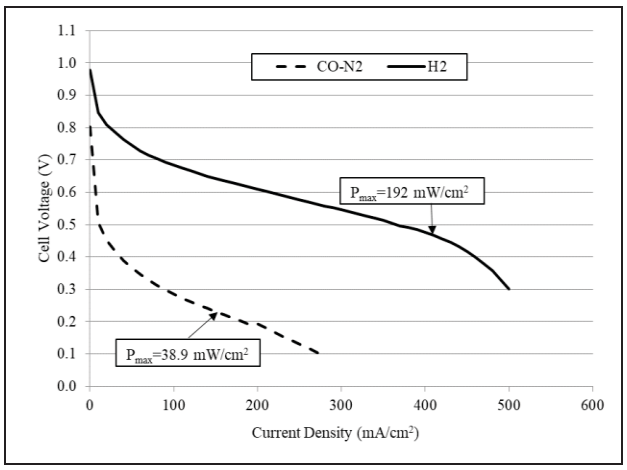

Fig. 10. The polarization curves of the Pt-Ru-Ni MEA fed with air: The effect of the fuel type at the operating temperature of 80°C.

Fig. 11 illustrates the impact of the operating temperature (80, 95, and 100°C) on the performance of the fuel cell when it is fueled with a mixture of CO and N_2 (20% and 80% volume-based, respectively, at the flow rate of 100 mlit/min) as the fuel and O_2 as the oxidant (the flow rate of 500 mlit/min). At low current densities, as expected, the performance of the cell improves with the increase in the operating temperature. At high operating temperatures, for high current densities, however, the voltage abruptly drops. This is reflected in the maximum power density of the fuel cell being 38.9, 37.3, and 36.1 mW/cm^2, respectively, when the operating temperature is 80, 95, and 100°C. To investigate this behavior, the same experiments were repeated but at the higher flow rates of the fuel and oxidant.

Fig. 12 depicts the polarization curves of the fuel cell at the operating temperatures of 95 and 100°C for two cases; the fuel and air flow rates of 100/500 and 250/1500 mlit/min. The figure indicates that with an increase in the flow rates (from 100 to 500 mlit/min for the anode flow rate and 500 to 1500 mlit/min for the cathode flow rate), the sudden drop of voltage at high current densities is avoided, which means the drop was due to the starvation of the electrodes (mainly the anode). Also, the curves in Fig. 12 show that the performance of the cell at 95°C is better than that at 100°C (the maximum power density of 44.0 vs 38.2. mW/cm^2, respectively, for 250/1500 mlit/min and 37.3 vs 36.1 mW/cm^2, respectively, for 100/500 mlit/min). This might be a result of the drying of the electrolyte membrane at extremely high operating temperatures.

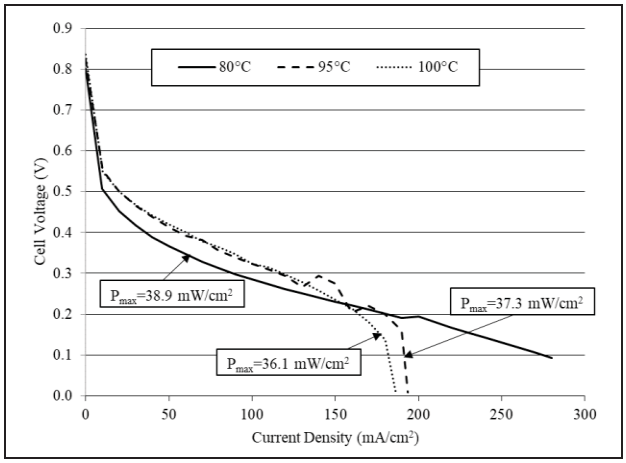

Fig. 11. The polarization curves of the Pt-Ru-Ni MEA fed with the mixture of N_2 and CO and air (100/500 mlit/min): The effect of the cell operating temperature.

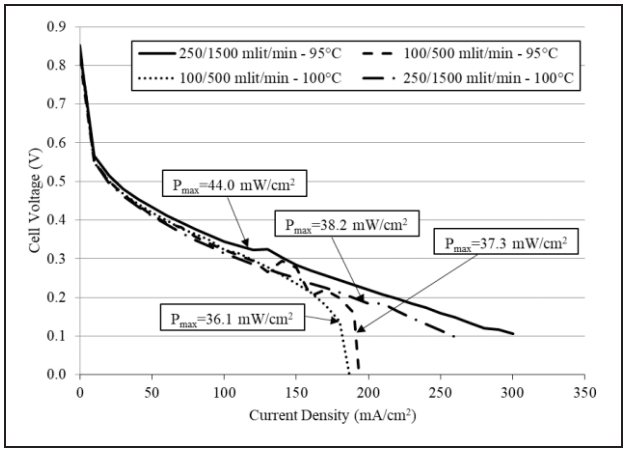

Fig. 12. The polarization curves of the Pt-Ru-Ni MEA fed with N_2-CO and air: The effect of the fuel and air flow rates.

If the maximum power density of the current MEA at 44 mW/cm^2 and those of the commercial DMFC (Pt-Ru), homemade Pt-Ru, and Pt-Sn are compared at similar operating conditions (CO-N_2/air and 95°C), 24.7 and 38.8 mW/cm^2, respectively, it can be concluded that in this operating condition, the current MEA outperformed both Pt-Ru catalysts. However, at this operating condition, the Pt-Ru-Ni MEA and unsupported Pt-Sn MEA performed similarly (44 vs. 43.8 mW/cm^2, respectively). It should be noted that at this operating condition, the maximum power density of the Pt-Ru-Ni MEA was twice as high as that of the unsupported Pt-Sn MEA. At the operating temperature of 80°C, the Pt-Ru-Ni MEA also outperformed the Pt-Ru MEAs, but it was inferior to the Pt-Sn MEA.

To sum up, when fueled with hydrogen, the Pt-Ru-Ni MEA cannot compete with Pt-Ru MEAs. When fueled with CO-containing fuels, the Pt-Ru-Ni MEA outperforms all the Pt-Ru MEAs but is outperformed by the Pt-Sn MEA. These findings are aligned with the results reported by Wang et al. (2006), Ye et al. (2007), and Martínez-Huerta et al. (2006) and contradict those reported by Pasupathi & Tricoli (2008). This discrepancy, as noted earlier, might be due to the different fabrication methods that were used to develop the MEAs in the latter research.

3.2.2. Pt-Ru-Sn-Ni Electrocatalyst

To further improve the performance of anode electrocatalysts, several attempts have been reported in the literature to fabricate quaternary Pt-based electrocatalysts and beyond, including Pt–Ru–Pd–Rh–Au (Mints et al., 2022), Pt-Ru-Mo-W (Choi et al., 2002), Pt-Ru-Os-Ir (Reddington et al., 1998), and Pt-Ru-Sn-W (Arico et al., 1995). In the previous experiments, it was shown that when Ni was added to Pt-Ru, the performance of the catalyst was improved. Also, it was observed that the Pt-Sn catalyst has the best performance for CO-containing fuels among all developed MEAs so far. Furthermore, Spinacé et al. (2005) reported that the carbon-supported Pt-Sn-Ni electrocatalyst has a better performance than that of the carbon-supported Pt-Sn electrocatalyst in direct ethanol fuel cells. All these observations indicate that the next logical step is to fabricate quaternary electrocatalysts containing platinum, ruthenium, tin, and nickel (Pt-Ru-Sn-Ni).

Fig. 13 illustrates the performance of the Pt-Ru-Sn-Ni MEA when fed with either hydrogen or carbon monoxide as the fuel and oxygen as the oxidant (100/200 mlit/min) at the operating temperature of 80°C. The ratio of the maximum power density of the fuel cell when fueled with hydrogen to that when fueled with carbon monoxide is 2.9 (95.7 vs 33.0 mW/cm^2). This ratio is much smaller for this catalyst compared to those of the previous ones. This indicates that the performances of the fuel cell when fed with hydrogen and carbon monoxide are getting closer but this does not necessarily mean that the fuel cell was performing better when fueled by CO but its performance got worse when fueled with hydrogen.

Fig. 14 depicts the polarization curves of the fuel cell when it was fueled with CO and O_2 (500/1000 mlit/min) at two operating temperatures, 80 to 95°C. The curves show that the performance of the fuel cell improves with an increase in the operating temperature, as expected. The maximum power density increases from 26.7 to 33.7 mW/cm^2 when the operating temperature increases from 80 to 95°C. The instability in the operation of the fuel cell at high temperatures should be also noted.

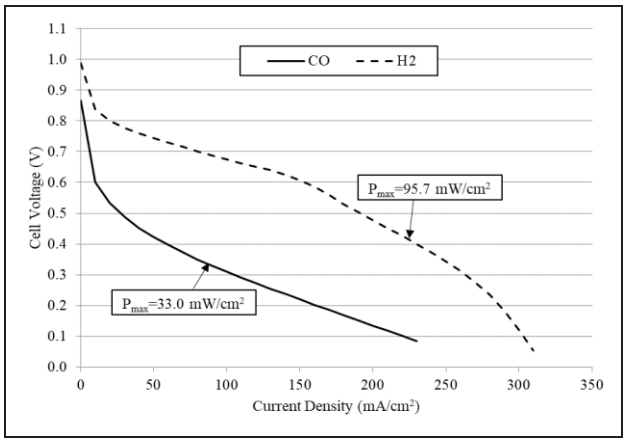

Fig. 13. The polarization curves of the Pt-Ru-Sn-Ni MEA fed with O_2 as the oxidant at the operating temperature of 80°C: The effect of the fuel type (H_2 and CO) (100/200 mlit/min).

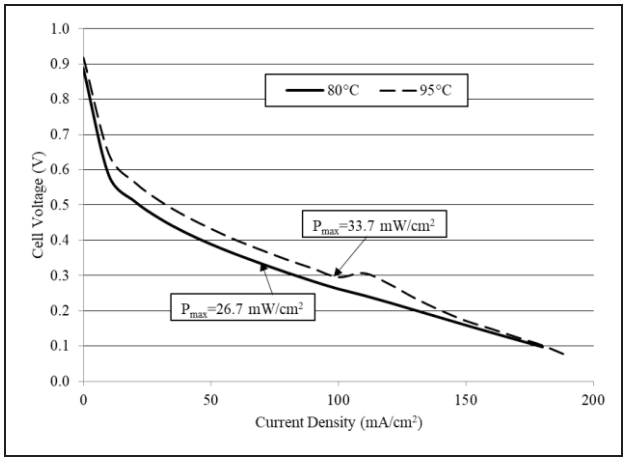

Fig. 14. The polarization curves of the Pt-Ru-Sn-Ni MEA fed with CO as the fuel and O_2 as the oxidant (500/1000 mlit/min): The effect of the operating temperature.

Fig. 15 shows the polarization curves of the fuel cell fed with CO and O_2 (100/200 mlit/min) at the operating temperature of 80°C. In these experiments, the humidification temperature of the cathode was 80°C and the humidification temperature of the anode was 80 and 90°C. The figure indicates that the performance of the fuel cell was slightly improved when the temperature of the humidification process was increased from 80 to 90°C from 33.0 to 34.0 mW/cm^2 (about 1.3% increase in the maximum power density).

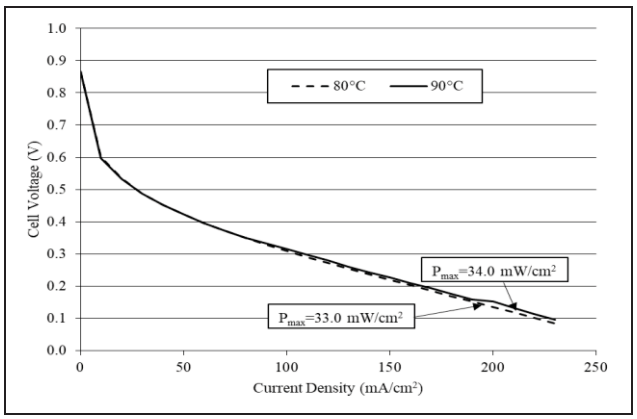

Fig. 15. The polarization curves of the Pt-Ru-Sn-Ni MEA fed with CO as the fuel and O_2 as the oxidant (100/200 mlit/min) at the operating temperature of 80°C: The effect of the anode humidification temperature.

At the operating temperature of 80°C when the MEAs were fed with CO and O_2, the maximum power densities of the Pt-Ru-Sn-Ni MEA, Pt-Ru MEA, Pt-Sn MEA, and Pt-Ru-Ni MEA were 33.0, 33.2, 59.4, and 47.4 mW/cm^2, respectively. A similar pattern can be seen when the fuel cells were fed with carbon monoxide and oxygen at the operating temperature of 80°C, where the Pt-Ru-Sn-Ni catalyst demonstrated the most inferior performance. When fueled with hydrogen, the Pt-Ru-Sn-Ni MEA had the lowest maximum power density among all the experiments conducted so far. Collectively, all these values indicate that contrary to the initial expectations, the Pt-Ru-Sn-Ni MEA was inferior compared to the other MEAs. The good performances observed in Pt-Ru, Pt-Sn, and Pt-Ru-Ni MEAs did not result in the exceptional performance of the Pt-Ru-Sn-Ni MEA.

3.2.3. Pt-Ru-Sn-Co Electrocatalyst

Mukherjee et al. (2022), Pasupathi & Tricoli (2008), Zhang et al. (2004), Antolini et al. (2006), and Moreno et al. (2009) all experimentally demonstrated that the addition of cobalt (Co) to Pt-Ru electrocatalyst can positively impact the catalytic activity of the electrocatalyst, particularly towards methanol oxidation. In an attempt to improve the anode catalyst, the Pt-Ru-Sn-Co electrocatalyst was developed and used as the catalyst in the MEA. The anode electrocatalyst was made of the Pt-Ru-Sn-Co with the loading of 6 mg/cm^2 and the cathode electrocatalyst was made of the carbon-supported platinum with the loading of 4 mg/cm^2 and Nafion® 117 as the electrolyte. Fig. 16 depicts the polarization curves for the fuel cell with the Pt-Ru-Sn-Co anode electrocatalyst at two operating temperatures of 80 and 95°C when the cell was fueled with the mixture of 20% CO and 80% N_2 as the fuel and air as the oxidant (250/1000 mlit/min). As with the other cases, the increase in the operating temperature improves the performance of the fuel cell, and the maximum power density increases from 25.8 to 30.6 mW/cm^2 when the operating temperature increases from 80 to 95°C.

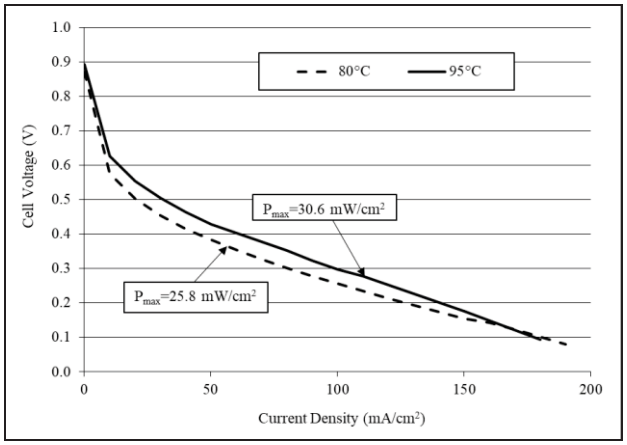

Fig. 16. The polarization curves of the Pt-Ru-Sn-Co MEA fed with CO-N_2 as the fuel and air as the oxidant: The effect of the operating temperature.

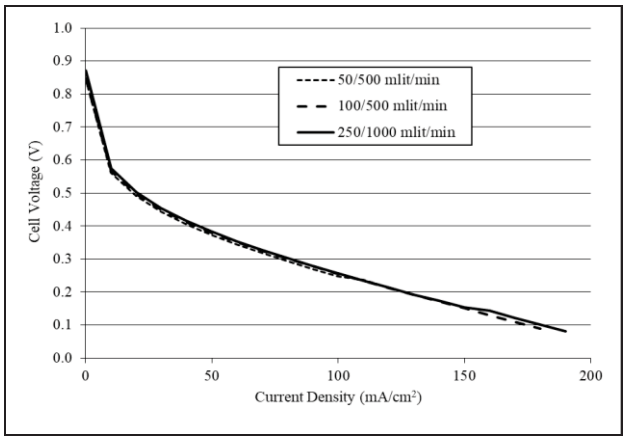

Fig. 17. The polarization curves of the Pt-Ru-Sn-Co MEA fed with CO-N_2 as the fuel and air as the oxidant: The effect of the reactant flow rates.

Fig. 17 illustrates the impact of the fuel and air flow rates on the performance of the fuel cell when it was fed with CO-N_2 (20% and 80%, respectively) as the fuel and air as the oxidant. The curves indicate that the performance of the fuel cell is mostly unaffected by the variation of the flow rates. In this figure, the maximum power density is in the range of 25.7 and 26.1 mW/cm^2.

At the operating temperature of 95°C when the fuel cells were fed with CO-N_2 (20% and 80%, respectively) and air, the maximum power densities of the Pt-Ru-Co-Sn, commercial and homemade Pt-Ru, Pt-Sn, and Pt-Ru-Ni MEAs are 30.6, 24.7, 38.8, 43.8, and 37.3 mW/cm^2, respectively. The performance of the Pt-Ru-Sn-Co and Pt-Ru-Sn-Ni MEAs are of the same magnitude. A similar trend is observed at the operating temperature of 80°C when the fuel cells were fed with CO-N_2 and air, however in this case the Pt-Ru-Sn-Ni MEA outperforms the Pt-Ru-Sn-Co MEA. All these values indicate that the Pt-Ru-Sn-Co MEA is inferior to the previous MEAs, except for the commercial Pt-Ru.

3.2.4. Pt-Ru-Sn-Co-W Electrocatalyst

Several research teams have reported that the addition of tungsten to catalysts can improve their activity. This can be achieved by forming Pt-W (Zhou et al., 2004; Ham et al., 2008), Pt-Ru-W (Zhou et al., 2004; Zhou et al., 2003), or Pt-Ru-Sn-W (Arico et al., 1995). As a last attempt to improve the performance of the MEA by manipulating the anode electrocatalyst, the Pt-Ru-Sn-Co-W electrocatalyst was developed and used as the anode catalyst for the MEA. The anode electrocatalyst was Pt-Ru-Sn-Co-W with the loading of 6 mg/cm^2. The cathode electrocatalyst and the electrolyte were similar to the previous MEAs.

First, several experiments at the operating temperature of 95°C were conducted to evaluate the impacts of fuel and oxidant types, i.e. CO-N_2 (20% and 80%, respectively) or CO and air or oxygen, on the performance of the MEA. Fig. 18 indicates that while the effect of using CO-N_2 or CO is negligible, the impact of the oxidant type is the dominant factor. As expected, the performance of the fuel cell was much better when fed with O_2 compared to that when fed with air. The maximum power density of the fuel cell when fed with O_2 was about 50% higher than that when fed with air. When fueled by CO, the maximum power density of the fuel cell with oxygen and air is 78.5 and 53.2 mW/cm^2, respectively. When fueled by CO, these values are 73.5 and 53.3 mW/cm^2, respectively. Considering a different point of view, when the oxidant is air, the maximum power density of the fuel cell with CO and CO-N_2 are 53.2 and 53.3 mW/cm^2, respectively. When the oxidant is oxygen, these values are 78.5 and 73.5 mW/cm^2, respectively. Similarly, Fig. 19 shows the polarization curves of the fuel cell when fueled with CO-N_2 and H_2 as the fuels and oxygen as the oxidant at the operating temperature of 80°C. The maximum power density when the fuel cell was fueled with hydrogen is about 5.1 times greater than that when it was fueled with CO-N_2 (320 vs 62.2 mW/cm^2). Fig. 20 depicts the polarization curves of the fuel cell when fed with CO-N_2 (20/80%) as the fuel and O_2 as the oxidant at two operating temperatures, 80 and 95°C. The figure shows that when the operating temperature was increased from 80 to 95°C, the maximum power density increased from 62.2 to 73.5 mW/cm^2.

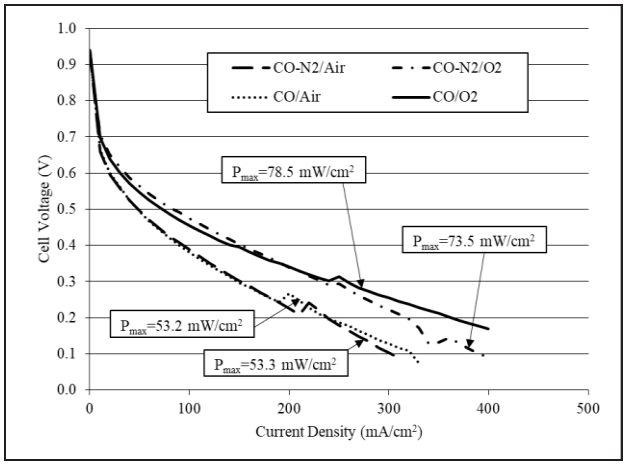

Fig. 18. The polarization curves of the Pt-Ru-Sn-Co-W MEA fed with CO-N_2 and CO as the fuels and air and O_2 as the oxidants at the operating temperature of 95°C: The effect of the reactant concentration on the fuel cell performance.

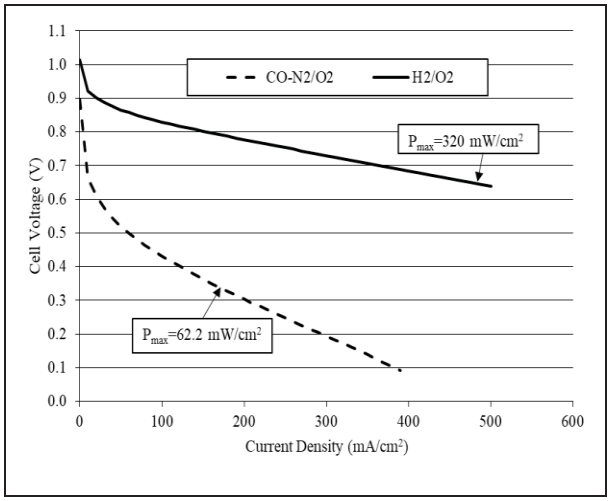

Fig. 19. The polarization curves of the Pt-Ru-Sn-Co-W MEA fed with CO-N_2 and H_2 as the fuels and O_2 as the oxidant at the operating temperature of 80°C: The effect of the fuel type.

On this particular MEA, a short-term (30 minutes) performance stability test was conducted where the current density was repeatedly switched between 10 and 250 mA/cm^2 and the cell voltage cycles were recorded. The results indicated that no degradation was evident in the short-term output stability experiment. Also, the experiment showed that increasing the cathode humidification temperature had a stronger effect on the performance than increasing the anode humidification temperature. This can be attributed to the significant thickness of the used membrane.

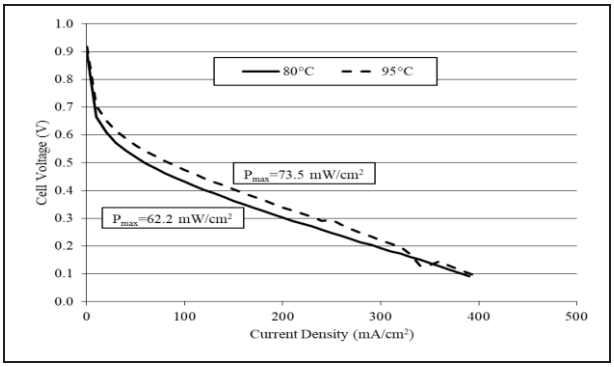

Fig. 20. The polarization curves of the Pt-Ru-Sn-Co-W MEA fed with CO-N_2 as the fuel and O_2 as the oxidant: The effect of the operating temperature.

At the operating temperature of 95°C when the fuel cells were fed with CO-N_2 and air, the maximum power densities of the Pt-Ru-Sn-Co-W, commercial and homemade Pt-Ru, Pt-Sn, Pt-Ru-Ni, Pt-Ru-Sn-Ni, and Pt-Ru-Co-Sn MEAs are approximately 53, 25, 39, 44, 44, 34, and 31, respectively. Clearly, the Pt-Ru-Sn-Co-W MEA has the highest power density at this operating condition among all the MEAs developed so far. Similarly, when the fuel cell was fed with CO-N_2 and oxygen at the operating temperature of 80°C, the maximum power density of Pt-Ru-Co-W-Sn MEA was higher than all the other MEAs. A similar trend can be observed when the MEAs were fed with hydrogen and oxygen at the operating temperature of 80°C. All these values indicate that the current MEA achieved the best performance among all the fabricated and tested MEAs so far.

3.3. Reducing The Thickness of The Electrolyte Membrane

Up to this point, the composition of anode electrocatalysts and the operating conditions of the cells were manipulated to achieve the best performance. In the rest of this paper, the impact of the electrolyte membrane thickness will be studied.

Electrolytes in MEAs have two major functions: to conduct ions between two electrodes and to prevent the direct mixing of the reactants. While using a thinner membrane can improve its ionic conductivity and thus the performance of the MEA, it can also increase fuel crossover, particularly for liquid fuels. Peighambardoust et al. (2010) listed the following advantages for thinner membranes:

- lower water crossover
- lower membrane ionic resistance
- higher membrane ionic conductivity
- lower cost
- faster hydration

They reported that lower durability and higher fuel bypass as the main problems of thinner membranes. For the rest of this work, one of the previously developed catalysts is redeveloped by employing a much thinner membrane.

3.3.1. Pt-Sn Electrocatalyst with Nafion® 212

For this MEA, the anode and cathode electrocatalysts were similar to the previously developed Pt-Sn MEA. But in this case, Nafion® 212 with a thickness of 50.8 micrometers (2 mil) is used instead of Nafion® 117 with a thickness of 183 micrometers (7.2 mil) to fabricate the MEA. Fig. 21 shows the effect of the operating temperature on the performance of the fuel cell. The operating temperatures of 60, 80, and 95°C were tested. The polarization curves show that generally, the increase in the operating temperature improves the performance of the fuel cell. However, at high current densities, the voltage of the fuel cell at the operating temperature of 95°C is less than that of the fuel cell at 80°C. This is also reflected in the maximum power densities of the cells when 117, 130, and 77 mW/cm^2 are recorded at the operating temperatures of 60, 80, and 95°C, respectively. This might be because of the drying of the membrane at high operating temperatures.

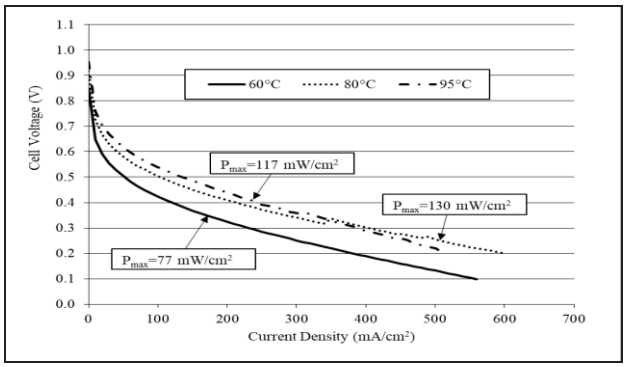

Fig. 21 The polarization curves of the Pt-Sn electrocatalyst with Nafion® 212 MEA fed with CO/O_2 (100/100 mlit/min): The effect of the operating temperature

Fig. 22 depicts the polarization curves of the fuel cell when fueled with CO and air at the operating temperature of 95°C at different flow rates of the fuel and the oxidant. It can be observed that increasing the flow rates from 100/200 to 500/1000 mlit/min significantly improves the performance of the fuel cell (the maximum power density of 85 vs. 119 mW/cm^2, respectively). But at high flow rates, increasing the flow rates from 500/1000 to 1000/2000 mlit/min slightly improves the performance of the fuel cell (the maximum power density of 119 vs. 128 mW/cm^2, respectively).

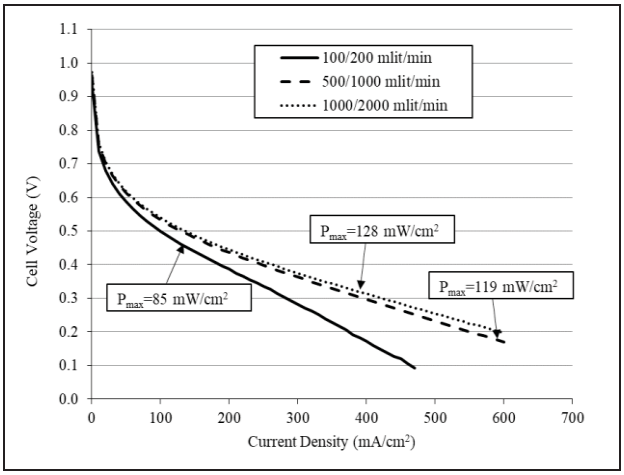

Fig. 22 The polarization curves of the Pt-Sn electrocatalyst with Nafion® 212 MEA fed with CO/air at the operating temperature of 95°C: The effect of the reactant flow rates

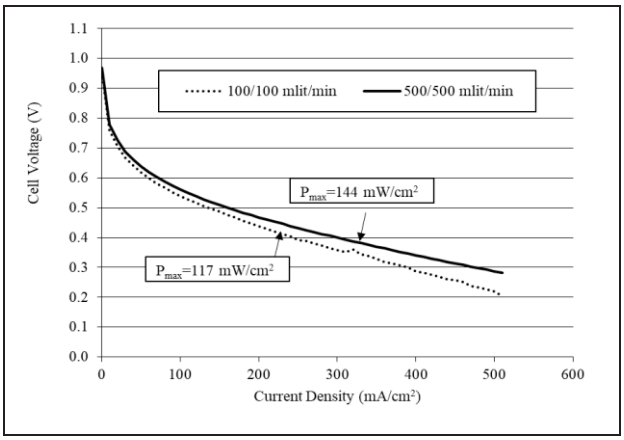

Fig. 23 The polarization curves of the Pt-Sn electrocatalyst with Nafion® 212 MEA fed with CO/O_2 at the operating temperature of 95°C: The effect of the reactant flow rates

Fig. 23 shows similar results when the MEA was fed with CO and O_2 at the operating temperature of 95°C. The curves demonstrate that when the flow rates of the fuel and the oxidant are increased from 100/100 to 500/500 mlit/min, the maximum power density of the fuel cell increases from 117 to 144 mW/cm^2.

Comparing the performance of the MEAs with the anode catalyst made of Pt-Sn and the electrolytes of Nafion® 117 and 212 membranes at the operating temperature of 80°C when fed with CO and O_2 indicates that the maximum power density of the latter is more than twice that of the former. A similar pattern can be observed when the MEA was fed with CO and air at the operating temperature of 95°C. In fact, the performance of the Pt-Sn electrocatalyst with Nafion® 212 membrane MEA was the best among all the MEAs that were developed and tested in this work.

4. CONCLUSION

The results of the experiments presented in this paper indicate that PEMFCs can be fueled with carbon monoxide-containing fuels if suitable anode electrocatalysts are used at the optimum operating conditions. Among various anode electrocatalysts that were studied, Pt-Ru-Sn-Co-W demonstrated the best performance. More specifically the following conclusions can be made from the presented experimental results:

- Direct alcohol fuel cells were used as the source of inspiration for the development of the anode catalysts. The results proved that this strategy was successful. All homemade MEAs used the carbon-supported Pt cathode catalyst and the Nafion® 117 membrane, except the last MEA that used Nafion® 212.
- The Pt-Sn anode catalyst significantly improved the performance of MEA when the cell was fueled with CO-containing fuels.
- For the Pt-Sn anode electrocatalyst, using carbon as the support for the anode catalyst deteriorated the performance of the MEA.
- The addition of nickel to the Pt-Ru catalyst to develop the Pt-Ru-Ni electrocatalyst improved the performance of the Pt-Ru catalysts when fueled with CO-containing fuels but could not compete with the Pt-Sn MEA.
- Two quaternary Pt-based electrocatalysts, i.e. Pt-Ru-Sn-Ni and Pt-Ru-Sn-Co, were developed and tested. The performance of both catalysts was inferior compared to previous MEAs.
- Unlike previously developed ternary and quaternary anode electrocatalysts, the Pt-Ru-Sn-Co-W anode catalyst demonstrated superior performance compared to all other MEAs made using the Nafion®117 membrane.
- Finally, the Pt-Sn MEA with the Nafion®212 membrane not only outperformed the Pt-Sn MEA with the Nafion®212 membrane but also was superior to all other MEAs with a very wide

margin. This indicates the critical importance of membrane thickness.
- The performance of all MEAs was improved when their operating temperature increased but the magnitude of improvement was different.
- The performance of the MEAs was improved by increasing the flow rates of the reactants; however, this improvement was limited to a certain level.
- Feeding the MEAs with CO typically provided better performance compared to that of CO-N_2. Similarly, O_2 rather than air as the oxidant provided better performance. However, the magnitude of the impact depended on other operating conditions.
- Some of the experiments indicated that DEFCs are closer to DCMFCs than other fuel cell types in terms of the similarity of the cell performance.

Overall, the results demonstrated that the performance of DCMFCs can be significantly improved by developing a suitable anode electrocatalyst, using a thinner membrane, and operating at optimum conditions. These results are not only applicable for DCMFCs but also are very useful for other PEMFCs operating with CO-containing fuels.

5. FUTURE WORK

The long-term steady-state and dynamic operation tests should be conducted on the best performing MEAs to evaluate the stability, longevity, and degradation rate of these MEAs. Due to their higher tolerance for CO, easier water management, easier thermal management, and less cooling load, and no need for external humidifiers, high-temperature PEMFCs are potentially suitable for this application and their performance should be investigated. When the single-cell units are optimized, the next step will be to fabricate fuel cell stacks and integrate the balance of the plant, including a dedicated gasifier.

ACKNOWLEDGEMENT

The authors would like to thank the American Science and Technology Corporation (AST) for sharing some of the data used in this paper.

REFERENCES

Ahn, C. Y., Kim, S., Choi, H. J., Lee, J., Kang, S. Y., Kim, O. H., ... and Cho, Y. H. (2022). Effect of iridium oxide as an additive on catalysts with different Pt contents in cell reversal conditions of polymer electrolyte membrane fuel cells. International Journal of Hydrogen Energy, 47(3), 1863-1873.

Antolini, E., Salgado, J. R., and Gonzalez, E. R. (2006). The methanol oxidation reaction on platinum alloys with the first row transition metals: the case of Pt-Co and–Ni alloy electrocatalysts for DMFCs: a short review. Applied Catalysis B: Environmental, 63(1), 137-149.

Antolini, E. (2007). Catalysts for direct ethanol fuel cells. Journal of Power Sources, 170(1), 1-12.

Aramata, A., and Masuda, M. (1991). Platinum Alloy Electrodes Bonded to Solid Polymer Electrolyte for Enhancement of Methanol Electro-oxidation and Its Reaction Mechanism. Journal of The Electrochemical Society, 138(7), 1949-1957.

Arico, A. S., Poltarzewski, Z., Kim, H., Morana, A., Giordano, N., and Antonucci, V. (1995). Investigation of a carbon-supported quaternary Pt Ru Sn W catalyst for direct methanol fuel cells. Journal of power sources, 55(2), 159-166.

Brkovic, S. M., Kaninski, M. P. M., Lausevic, P. Z., Saponjic, A. B., Radulovic, A. M., Rakic, A. A., ... and Nikolic, V. M. (2020). Non-stoichiometric tungsten-carbide-oxide-supported Pt–Ru anode catalysts for PEM fuel cells–From basic electrochemistry to fuel cell performance. International Journal of Hydrogen Energy, 45(27), 13929-13938.

Choi, W. C., Kim, J. D., and Woo, S. I. (2002). Quaternary Pt-based electrocatalyst for methanol oxidation by combinatorial electrochemistry. Catalysis Today, 74(3), 235-240.

Choi, J. H., Park, K. W., Kwon, B. K., and Sung, Y. E. (2003). Methanol oxidation on Pt/Ru, Pt/Ni, and Pt/Ru/Ni anode electrocatalysts at different temperatures for DMFCs. Journal of the Electrochemical Society, 150(7), A973-A978.

Choudhary, A. K., and Pramanik, H. (2020). Addition of rhenium (Re) to Pt-Ru/f-MWCNT anode electrocatalysts for enhancement of ethanol electrooxidation in half cell and single direct ethanol fuel cell. International Journal of Hydrogen Energy, 45(24), 13300-13321.

Chu, D., and Jiang, R. (2002). Novel electrocatalysts for direct methanol fuel cells. Solid State Ionics, 148(3), 591-599.

Colmati, F., Antolini, E., and Gonzalez, E. R. (2006). Effect of temperature on the mechanism of ethanol oxidation on carbon supported Pt, PtRu and Pt 3 Sn electrocatalysts. Journal of Power Sources, 157(1), 98-103.

Di, Q., Zhao, X., Zhu, W., Luan, Y., Hou, Z., Fan, X., ... and Zhang, J. (2022). Controllable synthesis of platinum–tin intermetallic nanoparticles with high electrocatalytic performance for ethanol e oxidation. Inorganic Chemistry Frontiers, 9(6), 1143-1151.

Dubau, L., Maillard, F., Chatenet, M., Cavaliere, S., Jiménez-Morales, I., Mosdale, A., and Mosdale, R. (2020). Durability of alternative metal oxide supports for application at a proton-exchange membrane fuel cell cathode—Comparison of

antimony-And niobium-doped tin oxide. Energies, 13(2), 403.

Eguiluz, K. I., Malpass, G. R., Pupo, M. M., Salazar-Banda, G. R., and Avaca, L. A. (2010). Synthesis, Characterization, and Electrocatalytic Activity toward Methanol Oxidation of Carbon-Supported Pt x−(RuO_2− M) 1− x Composite Ternary Catalysts (M= CeO_2, MoO_3, or PbO_x). Energy & Fuels, 24(7), 4012-4024.

Gao, W., Zhang, Z., Dou, M., and Wang, F. (2019). Highly dispersed and crystalline Ta2O5 anchored Pt electrocatalyst with improved activity and durability toward oxygen reduction: promotion by atomic-scale Pt–Ta2O5 interactions. ACS Catalysis, 9(4), 3278-3288.

Goel, J., and Basu, S. (2012). Pt-Re-Sn as metal catalysts for electro-oxidation of ethanol in direct ethanol fuel cell. Energy Procedia, 28, 66-77.

Gonzalez-Hernandez, M., Antolini, E., and Perez, J. (2020). CO tolerance and stability of PtRu and PtRuMo electrocatalysts supported on N-doped graphene nanoplatelets for polymer electrolyte membrane fuel cells. International Journal of Hydrogen Energy, 45(8), 5276-5284.

Götz, M., and Wendt, H. (1998). Binary and ternary anode catalyst formulations including the elements W, Sn and Mo for PEMFCs operated on methanol or reformate gas. Electrochimica Acta, 43(24), 3637-3644.

Grgur, B. N., Markovic, N. M., and Ross, P. N. (1998). Electrooxidation of H_2, CO, and H_2/CO mixtures on a well-characterized Pt70Mo30 bulk alloy electrode. The Journal of Physical Chemistry B, 102(14), 2494-2501.

Gurau, B., Viswanathan, R., Liu, R., Lafrenz, T. J., Ley, K. L., Smotkin, E. S., ... and Sarangapani, S. (1998). Structural and electrochemical characterization of binary, ternary, and quaternary platinum alloy catalysts for methanol electro-oxidation. The Journal of Physical Chemistry B, 102(49), 9997-10003.

Ham, D. J., Kim, Y. K., Han, S. H., and Lee, J. S. (2008). Pt/WC as an anode catalyst for PEMFC: Activity and CO tolerance. Catalysis Today, 132(1), 117-122.

Hang, H., Altarawneh, R. M., Brueckner, T. M., and Pickup, P. G. (2020). Pt/Ru–Sn oxide/carbon catalysts for ethanol oxidation. Journal of The Electrochemical Society, 167(5), 054518.

He, C., Kunz, H. R., and Fenton, J. M. (1997). Evaluation of Platinum-Based Catalysts for Methanol Electro-oxidation in Phosphoric Acid Electrolyte. Journal of the Electrochemical Society, 144(3), 970-979.

Ioroi, T., Fujiwara, N., Siroma, Z., Yasuda, K., and Miyazaki, Y. (2002). Platinum and molybdenum oxide deposited carbon electrocatalyst for oxidation of hydrogen containing carbon monoxide. Electrochemistry communications, 4(5), 442-446.

Jiang, L., Zhou, Z., Li, W., Zhou, W., Song, S., Li, H., ... and Xin, Q. (2004). Effects of treatment in different atmosphere on Pt3Sn/C electrocatalysts for ethanol electro-oxidation. Energy & Fuels, 18(3), 866-871.

Jiménez-Morales, I., Cavaliere, S., Dupont, M., Jones, D., and Roziere, J. (2019). On the stability of antimony doped tin oxide supports in proton exchange membrane fuel cell and water electrolysers. Sustainable Energy & Fuels, 3(6), 1526-1535.

Jusys, Z., Schmidt, T. J., Dubau, L., Lasch, K., Jörissen, L., Garche, J., and Behm, R. J. (2002). Activity of PtRuMeO x (Me= W, Mo or V) catalysts towards methanol oxidation and their characterization. Journal of Power Sources, 105(2), 297-304.

Kim, G. Y., Lee, J., Rho, Y. J., Kim, W. H., Kim, M., Ahn, J. H., and Ryu, W. H. (2022). Rhenium oxide/sulfide binary phase flakes decorated on nanofiber support for enhanced activation of electrochemical conversion reactions. Chemical Engineering Journal, 446, 136951.

Kurdin, K. A., Kuznetsov, V. V., Sinitsyn, V. V., Galitskaya, E. A., Filatova, E. A., Belina, C. A., and Stevenson, K. J. (2022). Synthesis and characterization of Pt-HxMoO3 catalysts for CO-tolerant PEMFCs. Catalysis Today, 388, 147-157.

Lamy, C., Rousseau, S., Belgsir, E. M., Coutanceau, C., and Léger, J. M. (2004). Recent progress in the direct ethanol fuel cell: development of new platinum–tin electrocatalysts. Electrochimica Acta, 49(22), 3901-3908.

Lasch, K., Jörissen, L., and Garche, J. (1999). The effect of metal oxides as co-catalysts for the electro-oxidation of methanol on platinum–ruthenium. Journal of Power Sources, 84(2), 225-230.

Latif, H., Wasif, D., Rasheed, S., Sattar, A., Rafique, M. S., Anwar, A. W., ... and Usman, A. (2020). Gold nanoparticles mixed multiwall carbon nanotubes, supported on graphene nano-ribbons (Au-NT-G) as an efficient reduction electrode for Polymer Electrolyte Membrane fuel cells (PEMFC). Renewable Energy, 154, 767-773.

Lee, J. K., Lee, J., Han, J., Lim, T. H., Sung, Y. E., and Tak, Y. (2008). Influence of Au contents of AuPt anode catalyst on the performance of direct formic acid fuel cell. Electrochimica Acta, 53(9), 3474-3478.

Lee, D. W., Choi, D., Lee, M. J., Jin, H., Lee, S., Jang, I., ... and Yoo, S. J. (2021a). Tailoring of Pt island RuO_2/C catalysts by galvanic replacement to achieve superior hydrogen oxidation reaction

and CO poisoning resistance. ACS Applied Energy Materials, 4(8), 8098-8107.

Lee, H., Park, S., and Kim, H. (2021b). Preparation of CO-tolerant PtRuNi/C ternary electrocatalyst having a composition gradient shell. Chemical Engineering Journal, 414, 128792.

Ley, K. L., Liu, R., Pu, C., Fan, Q., Leyarovska, N., Segre, C., and Smotkin, E. S. (1997). Methanol Oxidation on Single-Phase Pt-Ru-Os Ternary Alloys. Journal of the Electrochemical Society, 144(5), 1543-1548.

Li, W., Zhou, W., Li, H., Zhou, Z., Zhou, B., Sun, G., and Xin, Q. (2004). Nano-stuctured Pt–Fe/C as cathode catalyst in direct methanol fuel cell. Electrochimica Acta, 49(7), 1045-1055.

Li, G., and Pickup, P. G. (2006). The promoting effect of Pb on carbon supported Pt and Pt/Ru catalysts for electro-oxidation of ethanol. Electrochimica Acta, 52(3), 1033-1037.

Li, Y., Jiang, G., Yang, Y., Song, W., Yu, H., Hao, J., and Shao, Z. (2023). PtIr/CNT as anode catalyst with high reversal tolerance in PEMFC. International Journal of Hydrogen Energy.

Liang, J., Li, N., Zhao, Z., Ma, L., Wang, X., Li, S., ... and Li, Q. (2019). Tungsten-doped L10-PtCo ultrasmall nanoparticles as a high-performance fuel cell cathode. Angewandte Chemie International Edition, 58(43), 15471-15477.

Lin, R., Che, L., Shen, D., and Cai, X. (2020). High durability of Pt-Ni-Ir/C ternary catalyst of PEMFC by stepwise reduction synthesis. Electrochimica Acta, 330, 135251.

Lin, L. C., Kuo, C. H., Hsu, Y. H., Hsu, L. C., Chen, H. Y., Chen, J. L., and Pan, Y. T. (2022). High-performance intermetallic PtCo oxygen reduction catalyst promoted by molybdenum. Applied Catalysis B: Environmental, 317, 121767.

Litkohi, H. R., Bahari, A., and Gatabi, M. P. (2020). Improved oxygen reduction reaction in PEMFCs by functionalized CNTs supported Pt–M (M= Fe, Ni, Fe–Ni) bi-and tri-metallic nanoparticles as efficient electrocatalyst. International Journal of Hydrogen Energy, 45(43), 23543-23556.

Liu, L., Pu, C., Viswanathan, R., Fan, Q., Liu, R., and Smotkin, E. S. (1998). Carbon supported and unsupported Pt–Ru anodes for liquid feed direct methanol fuel cells. Electrochimica Acta, 43(24), 3657-3663.

Martínez-Huerta, M. V., Rojas, S., De La Fuente, J. G., Terreros, P., Pena, M. A., and Fierro, J. L. G. (2006). Effect of Ni addition over PtRu/C based electrocatalysts for fuel cell applications. Applied Catalysis B: Environmental, 69(1), 75-84.

Matsui, T., Fujiwara, K., Okanishi, T., Kikuchi, R., Takeguchi, T., and Eguchi, K. (2006). Electrochemical oxidation of CO over tin oxide supported platinum catalysts. Journal of power sources, 155(2), 152-156.

Mints, V. A., Pedersen, J. K., Bagger, A., Quinson, J., Anker, A. S., Jensen, K. M., ... and Arenz, M. (2022). Exploring the Composition Space of High-Entropy Alloy Nanoparticles for the Electrocatalytic H_2/CO Oxidation with Bayesian Optimization. ACS Catalysis, 12(18), 11263-11271.

Moore, C. E., Eastcott, J., Cimenti, M., Kremliakova, N., and Gyenge, E. L. (2019). Novel methodology for ex situ characterization of iridium oxide catalysts in voltage reversal tolerant proton exchange membrane fuel cell anodes. Journal of Power Sources, 417, 53-60.

Molochas, C., and Tsiakaras, P. (2021). Carbon monoxide tolerant Pt-based electrocatalysts for H_2-PEMFC applications: current progress and challenges. Catalysts, 11(9), 1127.

Moreno, B., Jurado, J. R., and Chinarro, E. (2009). Pt–Ru–Co catalysts for PEMFC synthesized by combustion. Catalysis Communications, 11(2), 123-126.

Mukerjee, S., Lee, S. J., Ticianelli, E. A., McBreen, J., Grgur, B. N., Markovic, N. M., ... and De Castro, E. S. (1999). Investigation of enhanced CO tolerance in proton exchange membrane fuel cells by carbon supported PtMo alloy catalyst. Electrochemical and Solid-State Letters, 2(1), 12-15.

Mukherjee, P., Patil, I. M., Lokanathan, M., Parse, H., Kakade, B., and Swami, A. (2022). Ru decorated Pt2CoNi/C nanoparticles as a proficient electrocatalyst for oxygen reduction reaction. Journal of Alloys and Compounds, 918, 165520.

Neto, A. O., Giz, M. J., Perez, J., Ticianelli, E. A., and Gonzalez, E. R. (2002). The electro-oxidation of ethanol on Pt-Ru and Pt-Mo particles supported on high-surface-area carbon. Journal of the Electrochemical Society, 149(3), A272-A279.

Pasupathi, S., and Tricoli, V. (2008). Effect of third metal on the electrocatalytic activity of PtRu/Vulcan for methanol electro-oxidation. Journal of Solid State Electrochemistry, 12(9), 1093-1100.

Peighambardoust, S. J., Rowshanzamir, S., and Amjadi, M. (2010). Review of the proton exchange membranes for fuel cell applications. International journal of hydrogen energy, 35(17), 9349-9384.

Pick, Š. (1999). On the electronic structure of surface Pt–Sn alloys. Surface Science, 436(1), 220-226.

Pillai, S. R., Sonawane, S. H., Gumfekar, S. P., Suryawanshi, P. L., Ashokkumar, M., and Potoroko, I. (2019). Continuous flow synthesis of nanostructured bimetallic Pt-Mo/C catalysts in milli-channel reactor for PEM fuel cell application. Materials Chemistry and Physics, 237, 121854.

Ravichandran, S., Bhuvanendran, N., Xu, Q., Maiyalagan, T., Xing, L., and Su, H. (2022). Ordered mesoporous Pt-Ru-Ir nanostructures as superior bifunctional electrocatalyst for oxygen reduction/oxygen evolution reactions. Journal of Colloid and Interface Science, 608, 207-218.

Reddington, E., Sapienza, A., Gurau, B., Viswanathan, R., Sarangapani, S., Smotkin, E. S., and Mallouk, T. E. (1998). Combinatorial electrochemistry: a highly parallel, optical screening method for discovery of better electrocatalysts. Science, 280(5370), 1735-1737.

Rousseau, S., Coutanceau, C., Lamy, C., and Léger, J. M. (2006). Direct ethanol fuel cell (DEFC): electrical performances and reaction products distribution under operating conditions with different platinum-based anodes. Journal of Power Sources, 158(1), 18-24.

Samjeské, G., Wang, H., Löffler, T., and Baltruschat, H. (2002). CO and methanol oxidation at Pt-electrodes modified by Mo. Electrochimica Acta, 47(22), 3681-3692.

Santiago, E. I., Camara, G. A., and Ticianelli, E. A. (2003). CO tolerance on PtMo/C electrocatalysts prepared by the formic acid method. Electrochimica Acta, 48(23), 3527-3534.

Santos, V. P., and Tremiliosi-Filho, G. (2003). Effect of osmium coverage on platinum single crystals in the ethanol electrooxidation. Journal of Electroanalytical Chemistry, 554, 395-405.

Sapkota, P., Lim, S., and Aguey-Zinsou, K. F. (2023). Platinum–tin as a superior catalyst for proton exchange membrane fuel cells. RSC Sustainability, 1(2), 368-377.

Shen, P. K., Chen, K. Y., and Tseung, A. C. (1995). Performance of CO-electrodeposited Pt-Ru/WO_3 electrodes for the electrooxidation of formic acid at room temperature. Journal of Electroanalytical Chemistry, 389(1-2), 223-225.

Simões, F. C., Dos Anjos, D. M., Vigier, F., Léger, J. M., Hahn, F., Coutanceau, C., ... and Kokoh, K. B. (2007). Electroactivity of tin modified platinum electrodes for ethanol electrooxidation. Journal of Power Sources, 167(1), 1-10.

Song, S. Q., Zhou, W. J., Zhou, Z. H., Jiang, L. H., Sun, G. Q., Xin, Q., … and Tsiakaras, P. (2005). Direct ethanol PEM fuel cells: the case of platinum based anodes. International Journal of Hydrogen Energy, 30(9), 995-1001.

Spasov, D. D., Ivanova, N. A., Pushkarev, A. S., Pushkareva, I. V., Presnyakova, N. N., Chumakov, R. G., ... and Fateev, V. N. (2019). On the influence of composition and structure of carbon-supported Pt-SnO_2 hetero-clusters onto their electrocatalytic activity and durability in PEMFC. Catalysts, 9(10), 803.

Spinacé, E. V., Linardi, M., and Neto, A. O. (2005). Co-catalytic effect of nickel in the electro-oxidation of ethanol on binary Pt–Sn electrocatalysts. Electrochemistry Communications, 7(4), 365-369.

Suffredini, H. B., Salazar-Banda, G. R., and Avaca, L. A. (2007). Enhanced ethanol oxidation on PbO_x-containing electrode materials for fuel cell applications. Journal of Power Sources, 171(2), 355-362.

Tian, H., Cui, X., and Shi, J. (2021). Emerging electrocatalysts for PEMFCs applications: Tungsten oxide as an example. Chemical Engineering Journal, 421, 129430.

Torres-Santillan, E., Capula-Colindres, S., Teran, G., Reza-San German, C. M., Flores, M. E., and Valencia, O. G. R. (2022). Synthesis of Pt-Mo/WMCNTs nanostructures reduced by the green chemical route and its electrocatalytic activity in the ORR. In Carbon Nanotubes-Recent Advances, New Perspectives and Potential Applications. IntechOpen.

Ueda, A., Yamada, Y., Ioroi, T., Fujiwara, N., Yasuda, K., Miyazaki, Y., and Kobayashi, T. (2003). Electrochemical oxidation of CO in sulfuric acid solution over Pt and PtRu catalysts modified with TaO_x and NbO_x. Catalysis today, 84(3), 223-229.

Vigier, F., Coutanceau, C., Hahn, F., Belgsir, E. M., and Lamy, C. (2004a). On the mechanism of ethanol electro-oxidation on Pt and PtSn catalysts: electrochemical and in situ IR reflectance spectroscopy studies. Journal of Electroanalytical Chemistry, 563(1), 81-89.

Vigier, F., Coutanceau, C., Perrard, A., Belgsir, E. M., and Lamy, C. (2004b). Development of anode catalysts for a direct ethanol fuel cell. Journal of Applied Electrochemistry, 34(4), 439-446.

Wang, Y., Fachini, E. R., Cruz, G., Zhu, Y., Ishikawa, Y., Colucci, J. A., and Cabrera, C. R. (2001). Effect of surface composition of electrochemically codeposited platinum/molybdenum oxide on methanol oxidation. Journal of the Electrochemical Society, 148(3), C222-C226.

Wang, Z. B., Yin, G. P., Zhang, J., Sun, Y. C., and Shi, P. F. (2006). Co-catalytic effect of Ni in the methanol electro-oxidation on Pt–Ru/C catalyst for direct methanol fuel cell. Electrochimica acta, 51(26), 5691-5697.

Wang, Z. B., Yin, G. P., and Lin, Y. G. (2007). Synthesis and characterization of PtRuMo/C nanoparticle electrocatalyst for direct ethanol fuel cell. Journal of Power Sources, 170(2), 242-250.

Wang, H., Gao, J., Chen, C., Zhao, W., Zhang, Z., Li, D., ... and Li, Y. (2023). PtNi-W/C with Atomically Dispersed Tungsten Sites Toward Boosted ORR in Proton Exchange Membrane Fuel Cell Devices. Nano-Micro Letters, 15(1), 1-19.

Xu, J., Hua, K., Sun, G., Wang, C., Lv, X., and Wang, Y. (2006). Electrooxidation of methanol on carbon nanotubes supported Pt–Fe alloy electrode. Electrochemistry communications, 8(6), 982-986.

Yang, H., Ko, Y., Lee, W., Züttel, A., and Kim, W. (2019). Nitrogen-doped carbon black supported Pt–M (M= Pd, Fe, Ni) alloy catalysts for oxygen reduction reaction in proton exchange membrane fuel cell. Materials Today Energy, 13, 374-381.

Yang, G., Zhang, Q., Yu, H., and Peng, F. (2021). Platinum-based ternary catalysts for the electrooxidation of ethanol. Particuology, 58, 169-186.

Ye, F., Chen, S., Dong, X., and Lin, W. (2007). Carbon nanotubes supported Pt-Ru-Ni as methanol electro-oxidation catalyst for direct methanol fuel cells. Journal of natural gas chemistry, 16(2), 162-166.

Zabihian, F., Davari, A., and Osei-Prempeh, G. (2023). Carbon monoxide-resistant anode catalysts for single-cell direct carbon monoxide fuel cells (DCMFCs): Platinum-ruthenium (Pt-Ru) anode electrocatalysts. International Journal of Renewable Energy Resources, In press.

Zhang, H., Wang, Y., Fachini, E. R., and Cabrera, C. R. (1999). Electrochemically codeposited platinum/molybdenum oxide electrode for catalytic oxidation of methanol in acid solution. Electrochemical and solid-state letters, 2(9), 437-439.

Zhang, X., Zhang, F., & Chan, K. Y. (2004). Preparation of Pt–Ru–Co trimetallic nanoparticles and their electrocatalytic properties. Catalysis Communications, 5(12), 749-753.

Zhang, X., Li, H., Yang, J., Lei, Y., Wang, C., Wang, J., ... and Mao, Z. (2021). Recent advances in Pt-based electrocatalysts for PEMFCs. RSC advances, 11(22), 13316-13328.

Zhang, X., Truong-Phuoc, L., Asset, T., Pronkin, S., and Pham-Huu, C. (2022). Are Fe–N–C electrocatalysts an alternative to Pt-based electrocatalysts for the next generation of proton exchange membrane fuel cells?. ACS Catalysis, 12(22), 13853-13875.

Zhao, Y., Fan, L., Ren, J., and Hong, B. (2014). Electrodeposition of Pt–Ru and Pt–Ru–Ni nanoclusters on multi-walled carbon nanotubes for direct methanol fuel cell. International Journal of Hydrogen Energy, 39(9), 4544-4557.

Zhou, W., Zhou, Z., Song, S., Li, W., Sun, G., Tsiakaras, P., and Xin, Q. (2003). Pt based anode catalysts for direct ethanol fuel cells. Applied Catalysis B: Environmental, 46(2), 273-285.

Zhou, W. J., Li, W. Z., Song, S. Q., Zhou, Z. H., Jiang, L. H., Sun, G. Q., ... and Tsiakaras, P. (2004). Bi-and tri-metallic Pt-based anode catalysts for direct ethanol fuel cells. Journal of Power Sources, 131(1), 217-223.